Nanotechnology measurements of the Young's modulus of polymeric materials

Nanotechnology measurements of the Young's modulus of polymeric materials

J D Caicedo[1], O G Pandoli[2], J D Hernandez[1,3] and M N Frota[1*]

[1] Postgraduate Metrology Programme. Metrology for Quality and Innovation. Pontifical Catholic University of Rio de Janeiro, Rio de Janeiro, 22451-900, BRAZIL
[2] Chemistry Department, Pontifical Catholic University of Rio de Janeiro, 22451-900, BRAZIL
[3] Research Group GIFOURIER. University Antonio Nariño, Puerto Colombia, COLOMBIA

* E-mail: Mauricio N. Frota <mfrota@puc-rio.br>

Abstract. Making use of atomic force microscopy (AFM) —known as the state-of-the-art technology for handling matter on an atomic and molecular scale—, this paper describes the use of a nanotechnology technique for characterizing properties of polymeric materials. AFM measurement on two materials (polyamide and polystyrene) allowed to compare the performance of two distinct multi-asperity adhesion models based on the JKR (Johnson-Kendall-Robert) and DMT (Derajaguin-Muller-Toporov) theories, when assessing the Young's Modulus (modulus of elasticity) of the investigated materials. Experimental results confirm that the JKR model processed through a MatLab algorithm produces more reliable results of the Young's Modulus than the DMT model built-in in the AFM software.

Keywords. Metrology; Atomic force microscopy; AFM; Polymeric materials; DMT model; JKR model.

1. Introduction

Atomic force microscopy is a material analysis technique, which consists of scanning the surface of a material sample with a probe, thus providing a topographic image with atomic resolution and mechanical/physicochemical mapping of some relevant properties of the materials comprising the sample. It is based on the atomic force microscope, which was conceived by its inventor, the Physicist Gerd Binnig, Nobel Prize laureated in 1986. By revolutionizing the state of the art in measurements of the normal force in micro and nanoscale, the technique qualifies for measurements of adhesion forces less than 1 μN between the cantilever's tip and the surface of the material sample being investigated.

The characterization of the physical, chemical, morphological, structural, magnetic, thermal, optical, electronic and mechanical properties of materials at the macro, micro, and nanoscales is of great importance for the research of materials for various applications. As known, nanotechnology is a state-of-the-art research field that relies on handling matter on an atomic and molecular scale. The use of different techniques such as laser scanning confocal microscopy (LSCM) [1], Raman Confocal Microscopy [2], energy diffraction spectroscopy (EDS) [3] is commonly used and well established for chemical analysis composition of row natural materials, polymers, and bio composite.

Nowadays, the nanoindentation is the convectional method for analysis of mechanical properties of materials at micro and nanoscale [4,5], while AFM has been accepted in the research of polymeric materials [6,7], and more significantly in soft materials [6,8,9]. AFM cantilever/tip can be used to determine, for small deformations of the soft sample (typically 2 - 10 nm) forces varying from 0.2 to about 100 nN/m [10-12].

Figure 1 illustrate a typical configuration of the atomic force microscopy technology, encompassing a laser light, a piezoelectric/flexible cantilever arm with a small radius tip, lenses and a photodetector. Critical in this technique, the cantilever tip is commonly fabricated from silicon or silicon nitride (Si3N4) and mounted with a spring [13].

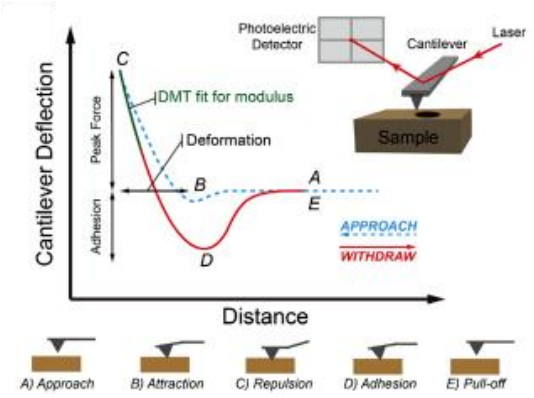

Figure 1. The typical configuration of the AFM technique [14]

According to the standard AFM procedure, the material sample to be studied is mounted on a piezoelectric base (sample scanner), free to move in three-dimensions [15]. The interaction between the sample and the tip generates forces (contact and non-contact forces), described by the law of Hook. Equation (1) defines the force F, expressed in terms of the material's constant k and the displacement Δl, measured at an equilibrium condition.

$$F = k\Delta l \tag{1}$$

The cantilever deflection caused by the contact and non-contact forces is measured by the photodetector, coupled to a laser beam passing through a lens, focused on the quadrants of the photodetector. The technique allows detection of the height (topography) and measurements of the load and adhesion forces. When measured separately, these forces generate force-displacement curves, which are interpreted by contact models.

Already buit-in in the processing software of the the atomic force microscope used, the Derjaguin-Muller-Toporov Model (DMT) calculates the modulus of elasticity (Young's Module) of many engineering materials from the AFM signal, providing reasonable results, except in the range of 0.5 to 10 GPa, where determination of the modulus of elasticity yields higher dispersions [10-12]. Dukukin [11,12] compared values of the modulus of elasticity measured by the AFM in its peak force tapping mode, for two different approaches: the Derjaguin-Muller-Toporov (DMT) [16] and the Johnson-Kendall-Robert (JKR) [17] theories. Both schemes rely on a spherical probe to perform the nanometric indentation depth. Their studies performed by measurements in polystyrene and polyurethanes samples, confirmed that the JKR model produces smaller dispersion and more reliable results, based on previously known reference values.

Making use of the AFM approach, the current study compares measurements results carried out in samples of polyamide and polystyrene, independently processed through the JKR and DMT models.

2. Theoretical background

Measurements of mechanical properties were performed by the AFM technique, in the peak force tapping mode (PF-TM), allowing the cantilever deflection and the z-piezo displacement curves to be obtained, over previously selected surface areas. The calculation of the elastic module based on the AFM and nanoindentation techniques evokes the Hertz model of contact between two smooth elastic bodies [18]. Essentially, the contact between a sphere and a surface can be modeled as an interaction between a probe and a sample, taking into account the probe-sample adhesion and the contact area. The elastic module nanoscales are, then, independently estimated by the DMT [16] and JKR [17] models.

2.1 The Derjaguin-Muller-Toporov Model (DMT)

Derjaguin, Muller and Toporov [16] —DMT model— describes a model of interaction between two spheres, modeled as a nondeformed ball in contact with a rigid plane. In this DMT model, the loading force is described by equation (2).

$$F_L = \frac{4}{3}E^*\sqrt{R^* d^3} + F_{adh} \tag{2}$$

where F_L is the loading force; F_{adh} the adhesion and R^* the radius of contact, given in equation (3).

$$\frac{1}{R^*} = \frac{1}{R_{indenter}} + \frac{1}{R_{surface}} \tag{3}$$

Associated with the DMT model, the modulus of elasticity (Young's Modulus) is calculated by Equation(4), where E^* is the contact modulus; υ and υ_{tip}, respectively, the Poison Ratio of the investigated material and of the probe tip.

$$E = (1 - {\upsilon_s}^2)\left[\frac{1}{E^*} - \frac{1 - {\upsilon_{tip}}^2}{E_{tip}}\right]^{-1} \tag{4}$$

2.2 The Johnson-Kendall-Robert Model (JKR)

Johnson, Kendall and Robert [17] —the JKR model— describes a model of interaction between two spheres, taking into account the influence of the surface energy on the contact point and the force of adhesion. Although not offering an explicit solution, it fits experimental force−indentation data, as discussed by Dukukin [11,12]. Following this line of thought, the loading force F_L is described by Equations (5), (6) and (7), where E^* is the contact modulus described by equation (8).

$$i(a) = \frac{a^2}{R^*} - \sqrt{\frac{2\pi W_{adh}}{E^*}} \tag{5}$$

$$W_{adh} = -\frac{2}{3}\left(\frac{F_{adh}}{\pi R^*}\right) \tag{6}$$

$$F_L(a) = \frac{4E^* a^3}{3R^*} - 2\sqrt{2\pi E^* W_{adh}\, a^3} \tag{7}$$

$$E^* = \left(\frac{1 + \sqrt[3]{16}}{3}\right)^{\frac{3}{2}} \frac{F_L}{\sqrt{R^* d^2}} \tag{8}$$

Following, $\boldsymbol{i(a)}$ is the indentation depth; a, the nominal radius of contact; R^*, the radius of contact, described by equation (3), while $\boldsymbol{W_{adh}}$ denotes the work of adhesion given by equation (6).

For the JKR model, the modulus of elasticity $\boldsymbol{E}$ is given by Equation (9), where υ is the Poison Ratio of the material investigated.

$$E = (1 - {\upsilon_s}^2)\left[\frac{1}{E^*}\right]^{-1} \tag{9}$$

2.3 Comparison of the DMT and JKR theories

Maugis [19] proposes a parameter λ —The Maguis parameter, defined in Equation (10) and ranging from 0 to ∞—, as a criterium to choose among the DMT and the JKR models, aiming to obtain greater accuracy in the calculation of the modulus of elasticity $\boldsymbol{E}$.

$$\lambda = \sigma_0\left[\frac{R^*}{W_{adh}E^{*2}}\right]^{\frac{1}{3}} \tag{10}$$

In this Equation, σ_0 is the limiting surface stress. More conveniently for soft materials, the parameter α —varying from 0 to 1—, also proposed by Maugis, allows to choose the more suitable model to be used; i.e.: the DMT (when α tends to 0) or the JKR Models (when α tends to 1), therefore refining his criterium for choosing which models suits better to assess the adhesion force [11,12,19,20].

$$\alpha = -\frac{50}{51}\left(e^{-\frac{250\lambda}{231}} - 1\right) \tag{11}$$

3. Materials and methods

Properties of the polymeric materials (polyamide and polystyrene) investigated are given in Table 1.

Table 1. Properties of the materials investigated

Material	Type	Poisson Ratio (1) (dimensionless)	Elastic Modulus (2) (GPa)
Polystyrene	Film	0.38	2.7
Polyamide	Vestamid- NRG 2101	0.41	1.8

(1) Reported by [20, 38]

(2) Nominal value reported by the Manufacturer

Three samples were used in the performed tests, one of polystyrene (0.7 mm thick, provided by the Bruker Corporation) and two of polyamide (0.5 mm and 1.2 mm, obtained from commercially available material used in the oil industry, mounted on a metallic coupon using an epoxy adhesive [21]). Figure 2 illustrates the tested samples submitted to the AFM technique.

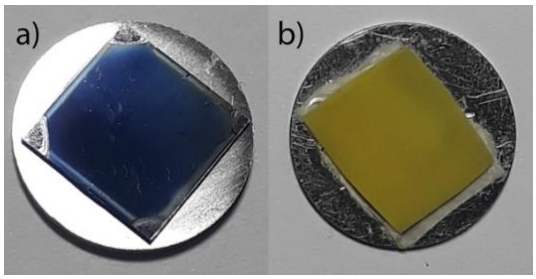

Figure 2. Image 2a: standard polystyrene by Bruker and 2b: polyamide VESTAMID® NRG 2101

Measurements were performed by the AFM Bruker multimode, version 8, which generates high quality images of the topography and reliable measurements of the mechanical properties at nano and microscale. The overall system uses a nano scope V type controller and a nanoscope software, versions 7.3 and 8.1. All measurements performed were carried out under ambient room temperature (T = 23 ºC), keeping the relative humidity in the 40 - 60 % range. During experiments, the standard cantilever was set for a normal operation in the open-air environment, using the peak force tapping quantitative nano-mechanics (PF-QNM) mapping, at 0.5 - 2 Hz of Z-piezo frequency. The physical properties of the probe and of the cantilever tip were determined using the absolute calibration method described in [22]. All AFM images were generated for a 2x2 µm scan size; scan rate: 0.998 Hz and 256 samples/line. Probe used: RTESPA-525, with nominal resonance frequency of 525 kHz, nominal tip radius of 8 nm, nominal spring constant of 200 N/m and side angle of 17.5° [23]. Cantilever tip effective radius = $32.22 \pm 3.56\ nm$; spring constant $K_s = 178 \pm 21.2\ N/m$; Deflection sensitivity $Ds = 63.11 \pm 4.75\ nm/V$.

4. Results and discussion

This section describes measurements performed on the polystyrene and polyamide material samples above characterized, making use of the atomic force microscope (AFM), operated in the peak force QNM imaging mode.

4.1 Polyamide and polystyrene: preparation of samples and AFM measurements

Independently calculations of the modulus of elasticity were performed and compared, based on the data generated by the atomic force microscope, whose output was further processed through the DMT and JKR models. First, the samples were scanned within a zone area delimited by 2 x 2 µm. Following the

standard operation procedure, the scan was performed within an area displaying fewer defects, confined within a much higher resolution of 500 x 500 nm. This means that a total number of 65536 (= 256 x 256) measurements were performed for each zone area scanned, therefore generating a huge amount of data points, for each one of the repeats 6, for polyamide and polystyrene. In the sequence, repeated values of the modulus of elasticity were directly obtained from the AFM measurements, through both DMT and JKR models. While the DMT output image is directly generated by the AFM output signal, the JKR image is processed through a Matlab algorithm, using the AFM raw data. Figures 3 and 4 shows, respectively, experimental results associated with AFM tests carried out.

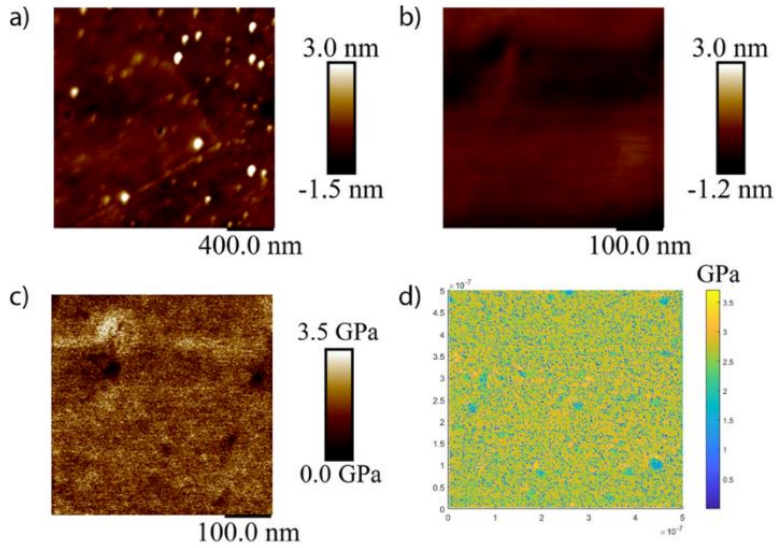

Figure 3. Surface AFM topography of the polystyrene film: (a) 2 x 2 µm; (b) 500 x 500 nm; Young's Modulus: (c) through the DMT model and (d) through the JKR model.

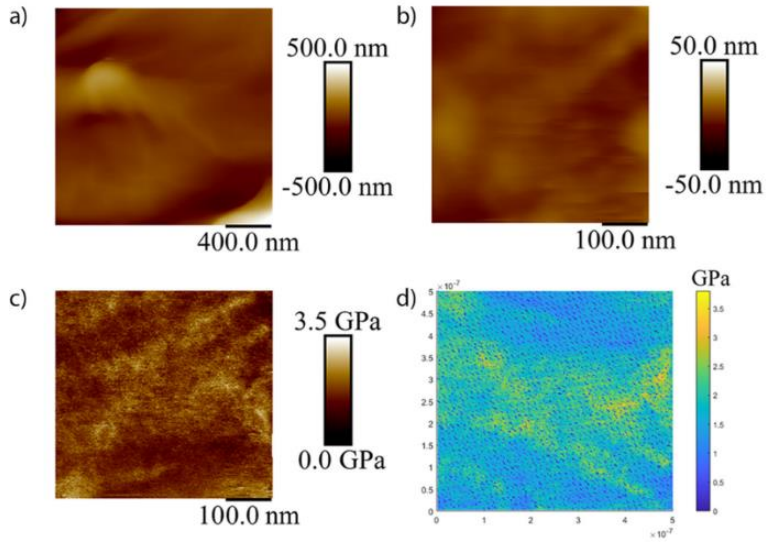

Figure 4. Surface AFM topography of the polyamide film (a) 2 x 2 µm; (b) 500 x 500 nm; Young's Modulus through (c) DMT model and (d) JKR model.

In Figures 3 and 4, the images 3a refers to topographic mapping within a 2 x 2 µm zone area of the sample; images 3b shows a magnification of the same image within a much narrower area (500 x 500

nm); images 3c shows an AFM image illustrating the quantitative mapping of the modulus of elasticity generated by the atomic force microscope, calculated through the DMT approach. Differently from the previous images, images 3d were not directly generated by the atomic microscope, but rather produced by a high-performance interactive algorithm developed in Matlab. This tool was used to calculate the modulus of elasticity and to plot the correspondent quantitative mapping, based on the alternative JKR Model. To make the JKR calculation possible, an on-line extraction software (Gwyddion 2.53) processed the AFM data as an input for a new round of calculation of the modulus of elasticity.

Table 2 summarizes the final results obtained for calculations of the Maugis α parameter and AFM measurements of the modulus of elasticity, based on the DMT and JKR models, the latter processed through the Matlab software. Just as an additional reference, Table 2 also reports a nominal value for the Polystyrene (1,6 ± 0,4 GPa) identified in the specialized literature [11, 12], whose metrological reliability was not clearly stated.

Table 2. Comparison of elastic modulus results: nominal *versus* DMT and JKR values

Material Tested	Nominal values provided by material manufacturers	Measured values reported in the specialized literature [20,21]			Measured by the Atomic Force Microscope (AFM),current study				
		α Parameter Equation (11)	Elastic Modulus		α Parameter Equation (11)	Elastic Modulus measured through the DMT model	DMT deviation from the nomial value	Elastic Modulus measured through the JKR model	JKR deviation from the nomial value
			DMT	JKR					
	(GPa)	(dimensionless)	(GPa)	(GPa)	(dimensionless)	(GPa)	(%)	(GPa)	(%)
Polystyrene	2.7	0.96	1.6 ± 0.4	2.7 ± 0.5	*0.98	1.754 ± 0.029	35.0	2.541 ± 0.042	5.9
Polyamide	1.8	-	-	-	*0.98	1.192 ± 0.013	33.8	1.680 ± 0.018	6.7

*For both materials, the value of the Alpha Parameter differs only in the fourth decimal place.

The fact that the Maugis α parameter approaches the value of 1 is a clear confirmation that the JKR approach is the model that better suits the calculation scheme to assess the value of the modulus of elasticity. As shown in Table 2, calculations of the modulus of elasticity through the JKR models reproduces the nominal value within less than 7%, while calculations through the DMT model differs from the manufacturers' values substantially (> 30%). While supporting the JKR model, the overall results of the study suggest that the DMT model is not suitable for characterizing both materials.

4.2 Expressing the uncertainty associated with AFM measurements

As distinctly stated in the international Vocabulary of Metrology (JCGM:2012), measurement uncertainty comprises, in general, many components. Some of these may be evaluated by Type A measurement uncertainty from the statistical distribution of the quantity values from a series of measurements can be characterized by standard deviations, as described by Equation (12).

$$u_A = \frac{S}{\sqrt{n}} = \sqrt{\frac{1}{n}\sum_{k=1}^{n}(x_i - \bar{x})^2} \tag{12}$$

Where u_A denotes the Type A component of the uncertainty associated with the AFM measurements performed, i.e.: the stochastic component calculated from the standard deviation (STDEV) S of the "n" measurements actually performed, understood as replicates of each measurement. The other components, which may be evaluated by Type B —components of measurement uncertainty determined by means other than a Type A evaluation of measurement uncertainty—can also be characterized by standard deviations, evaluated from probability density functions based on experience or other information.

However, considering the expressive mass of data that results from experiments carried out by the AFM technique, the following aspects should be considered before assessing the expanded uncertainty associated with the determination of the modulus of elasticity:

- the value measured by each interaction of the cantilever with the material sample allows to determine a "local value" of the modulus of elasticity, i.e.: measured in a single pixel of the 65536 pixels of the demarcated area (500 nm x 500 nm) in the material sample submitted to analysis by

the atomic force microscopy technique;

- after finalizing a complete cantilever scan over the demarcated area in the sample (i.e.: over 65536 measurement points), the AFM equipment will have generated 65536 independent measurements ("local values") of the modulus of elasticity (E), one for each pixel of this demarcated area (500 nm x 500 nm). Important, however, to keep in mind that, at the end of this first AFM cantilever scan over the sample surface, the value of the Type A uncertainty, calculated through equation (12), would be zero, since each of the 65536 points was measured just once.

Thus, in order to ensure reliability of the measurement and, consequently, to be able to associate an uncertainty value to each of these "local" independent measurement results, it is necessary to carry out replicates of the cantilever scan over the same demarcated area of the material sample. In the present study (polystyrene and polyamide), six replicates (six scans) were performed in the same demarcated area of the material samples, whose nominal values of the modulus of elasticity were previously provided by their manufacturers. By repeating the scan six times, it becomes possible to calculate the standard deviation and, therefore, the Type A component of the associated uncertainty (n = 6, Eq. 12).

Using the AFM technique, the modulus of elasticity was determined for each one of the 65536 points demarcated on the surface of the material sample studied, allowing to assess the value of the Type A uncertainty associated with each "local value" of the modulus of elasticity, calculated through Equation (12). In the present study, however, due to the absence of the AFM equipment calibration certificate, only the component of the uncertainty associated with the resolution of the AFM instrument was considered as the Type B uncertainty. Considering the resolution defined by the algorithm built-in in the AFM software (10^{-6} GPa), the u_B component of the uncertainty becomes $u_B = 2.88675\text{E-}07$, calculated through Equation (13).

$$u_B = \frac{(AFM\ Resolução)}{2\sqrt{3}} \tag{13}$$

In the sequence, the combined uncertainty is calculated by Equation (14)

$$u_C = \sqrt{u_A^2 + u_B^2} \tag{14}$$

While the expanded uncertainty, is calculated by Equation (15):

$$U = k * u_c \tag{15}$$

In this expression, k denotes the coverage factor, for a confidence level (1-α) of 95.0% (or, for a significance level of α = 5%). This k value is calculated taking into account the probability associated with the *t-Student* distribution and the number of degrees of freedom ($r = n - 1$, for 6 replicates, i.e.: 5 degrees of freedom) n), yielding k = 2.57.

Table 3 summarizes the results of all AFM measurements performed of the modulus of elasticity and their associated uncertainties. The combined (Type A and Type B) measurement uncertainty associated with the final values were assessed in compliance with the classical ISO/GUM approach [24]. Considering the huge amount of AFM data considered in the uncertainty analysis —six replicates of 65536 measurement points (256 x 256 pixels)—, Appendix A only reports an extract of the full AFM data sheet for each one of the materials investigates (polystyrene and polyamide).

Table 3. Synthesis of the measurement uncertainty associated with the modulus of elasticity

Sample Material	Points per replicate	Replicates	Average value	Standard Deviation	Standard uncertainty		Combined uncert.	Expanded uncert.
					u_A	u_B	$u_C = \sqrt{u_A^2 + u_B^2}$	$U = k * u_C$
	n	-	(GPa)	(GPa)	(GPa)	(GPa)	(GPa)	(GPa)
Polyamide (JKR)	65536*	6	1.680050	0.016379	0.006687	0.000028	0.0067	**0.018**
Polyamide (DMT)			1.192079	0.011600	0.004736	0.000028	0.0047	**0.013**
Polystyrene (JKR)	65536 *	6	2.540754	0.039917	0.016296	0.000028	0.0163	**0.042**
Polystyrene (DMT			1.753977	0.027428	0.011197	0.000028	0.0112	**0.029**

k (Coverage Factor) = 2.57, for a confidence level of 95% [ISO GUM 2008]

*Total number of measurements (256 x 256 = 65536), performed in six replicates

Due to space limitations, and as an example, these data table extracts were presented only for the JKR model, which produces more reliable results. As shown, at the end of these extracts, are shown the average values for each one of the six replicates, whose average of the average (six replicates, totalizing 393216 measurement results) certainly is the value that better represents the value of the modulus of the elasticity of the material sample studied. Regarding the calculation of the type A component of uncertainty, this was calculated based on the standard deviation of the six averages of the 65536 measurements made for each of the six replicates (n = 6). Table 3 summarizes the final results of this long-winded calculation.

5. Conclusion

Experimental results obtained during the implementation stage of the Atomic Force Microcopy Laboratory of Catholic University of Rio de Janeiro, confirm the efficacy of the atomic force microscopy technique used as a metrological tool for characterization of polymeric materials in the stress-strain regime. Systematic AFM measurements carried out in samples of two different materials (polystyrene and polyamide), operated in the peak force tapping mode, confirmed that, among the two models investigated (DMT and JKR), the latter approaches closely the previously known nominal value provided by the material sample manufacturers and produces smaller dispersion, therefore more suitable for assessing the modulus of elasticity of the investigated polymeric materials.

The atomic force microscopy proved to be an extremely promising technique to be used as a metrological tool of practical and scientific interest for material characterization, therefore capable of mapping the surface morphology and assessing physical properties (e.g.: Young's Module) of engineering materials. However, concerning the metrological reliability of the technique, a more robust analysis of the uncertainties associated with AFM measurements requires access to the AFM equipment calibration certificate (unfortunately, rarely supplied when purchasing AFM equipment), thus satisfying the unequivocal condition of traceability to the international system of units (SI).

6. Acknowledgments

Due to the *National Research Council of Brazil* (CNPq) (Grant 458302/2013-9) for the implementation of the AFM Laboratory and to the *Coordination for the Improvement of Higher Education Personnel* (CAPES), for the financial support (Master and Doctoral scholarships) provided to the first author.

References

[1] M. Minsky, *Memoir on Inventing the Confocal Scanning Microscope*, Scanning, vol. 10, no. 1 988, pp. 128–138, 1987.

[2] M. E. Andersen and R. Z. Muggll, *Microscopical techniques in the use of the molecular optics laser examiner Raman microprobe*, Anal. Chem., vol. 53, no. 12, pp. 1772–1777, 1981.

[3] G. A. Cox, Fundamentals of Energy Dispersive X-ray Analysis, Phys. Bull., vol. 36, 8, pp. 349–349, 1985.

[4] A. C. Fischer-Cripps, *Methods of correction for analysis of depth-sensing indentation test data for spherical indenters*, J. Mater. Res., vol. 16, no. 1, pp. 2244–2250, 2001.

[5] A. C. Fischer-Cripps, *Critical review of analysis and interpretation of nanoindentation test data*,

Surf. Coatings Technol., vol. 200, no. 14–15, pp. 4153–4165, 2006.
[6] I. W. Frank, D. M. Tanenbaum, A. M. van der Zande, and P. L. McEuen, *Mechanical properties of suspended graphene sheets*, J. Vac. Sci. Technol. B Microelectron. Nanom. Struct., vol. 25, no. 6, p. 2558, 2007.
[7] X. Cheng, K. W. Putz, C. D. Wood, and L. Brinson, *Characterization of local elastic modulus in confined polymer films via AFM indentation*, Macromol. Rapid Commun, vol. 36, no 4, pp. 391-397, 2015.
[8] M. Li, *Mapping Membrane Proteins on Cell Surface by AFM, in Investigations of Cellular and Molecular Biophysical Properties by Atomic Force Microscopy Nanorobotics,* Springer, Singapore, 2017, pp. 65–77.
[9] D. Biggs, H. Liu, D. Tirrell, and G. Ravichandran, *Modeling of atomic force microscope contact experiments on escherichia coli bacteria cellular systems, in Mechanics of Biological Systems & Micro-and Nanomechanics*, vol. 4, Springer, Cham, 2019, pp. 45–46.
[10] G. Smolyakov, S. Pruvost, L. Cardoso, B. Alonso, E. Belamie, and J. Duchet-Rumeau, *AFM PeakForce QNM mode: Evidencing nanometre-scale mechanical properties of chitin-silica hybrid nanocomposites*, Carbohydr. Polym., vol. 151, pp. 373–380, 2016.
[11] M. E. Dokukin and I. Sokolov, *Quantitative mapping of the elastic modulus of soft materials with HarmoniX and PeakForce QNM AFM modes*, Langmuir, vol. 28, no. 46, pp. 16060–16071, 2012.
[12] M. E. Dokukin and I. Sokolov, *On dependence of rigidity modulus on depth in nanoindentation experiments of homogeneous materials, Macromolecules*, vol. 45, no. 10, pp. 4277–4288, 2012.
[13] N. Jalili and K. Laxminarayana, A review of atomic force microscopy imaging systems: Application to molecular metrology and biological sciences, Mechatronics, vol. 14, no. 8, pp. 907–945, 2004.
[14] Y. F. Niu, Y. Yang, S. Gao, and J. W. Yao, *Mechanical mapping of the interphase in carbon fiber reinforced poly(ether-ether-ketone) composites using peak force atomic force microscopy: Interphase shrinkage under coupled ultraviolet and hydro-thermal exposure*, Polym. Test. vol. 55, 257–260, 2016.
[15] S. Liu and Y. Wang, *Application AFM in microbiology: A review Scan*, vol. 32, no. 2, 61–73, 2010.
[16] B. Derjaguin, V. Muller, and Y. Toporov, *Effect of contact deformation on the adhesion of elastic solids*, J. Colloid. Interface Sci, vol. 53, no. 2, pp. 314–326, 1975.
[17] K. L. Johnson, K. Kendall, and A. D. Roberts, *Surface Energy and the Contact of Elastic Solids*, Proc. R. Soc. A Math. Phys. Eng. Sci., vol. 324, no. 1558, pp. 301–313, 1971.
[18] H. Hertz, *Miscellaneous papers, Macmillan Co.*, p. 146, 1896.
[19] D. Maugis, *Adhesion of spheres: The JKR-DMT transition using a dugdale model*, J. Colloid Interface Sci., vol. 150, no. 1, pp. 243–269, 1992.
[20] H. K. Nguyen, S. Fujinami, and K. Nakajima, *Elastic modulus of ultrathin polymer films characterized by atomic force microscopy: The role of probe radius*, Polymer (Guildf), vol. 87, pp. 114–122, 2016.
[21] N. Sato, T. Kurauchi, S. Sato, and O. Kamigaito, *Mechanism of fracture of short glass fibre-reinforced polyamide thermoplastic*, J. Mater. Sci., vol. 19, no. 4, pp. 1145–1152, 1984.
[22] Y. Hua and D. Ph, PeakForce-QNM Advanced Applications Training, in Buker AFM training, 2014.
[23] Bruker, *RTESPA-525, AFM probes*, 2016. [Online]. Available in:
https://www.brukerafmprobes.com/p-3915-rtespa-525.aspx. [Accessed: 01-Jul-2019].
[24] GUM, I. (2008). *Guide to the Expression of Uncertainty in Measurement*, (1995), with Supplement 1, Evaluation of measurement data, JCGM 101: 2008. International Organization for Standardization, Geneva, Switzerland.

Appendix A. Extracts of the AFM measurement data

A1. Polyamide material: AFM measurement of the modulus of elasticity (GPa)

n	Replicate 1 (GPa)	Replicate 2 (GPa)	Replicate 3 (GPa)	Replicate 4 (GPa)	Replicate 5 (GPa)	Replicate 6 (GPa)	Average Value (GPa)	Standar Deviation (GPa)	u_A (GPa)	u_B (GPa)	$u_C = \sqrt{u_A^2 + u_B^2}$ (GPa)	$U = k * u_C$ (GPa)
1	1.546296	1.543294	1.559812	1.514773	1.548443	1.545630	1.543041	0.015013	0.006129	0.000028	0.00613	0.016
2	1.138955	1.136759	1.148935	1.115719	1.140469	1.138412	1.136541	0.011063	0.004517	0.000028	0.00452	0.012
3	1.331875	1.329297	1.343627	1.304704	1.333705	1.331287	1.329082	0.012961	0.005291	0.000028	0.00529	0.014
4	1.146567	1.144368	1.156548	1.123145	1.148177	1.146023	1.144138	0.011140	0.004548	0.000028	0.00455	0.012
5	0.961167	0.959347	0.969562	0.941585	0.962463	0.960758	0.959147	0.009323	0.003806	0.000028	0.00381	0.010
6	0.775804	0.774297	0.782594	0.759998	0.776879	0.775466	0.774173	0.007530	0.003074	0.000028	0.00307	0.008
7	1.157987	1.155781	1.168153	1.134376	1.159598	1.157532	1.155571	0.011256	0.004595	0.000028	0.00460	0.012
8	0.972586	0.970760	0.981074	0.952816	0.973977	0.972175	0.970565	0.009421	0.003846	0.000028	0.00385	0.010
9	0.976393	0.974564	0.984974	0.956529	0.977784	0.975980	0.974371	0.009477	0.003869	0.000028	0.00387	0.010
10	0.980199	0.978368	0.988780	0.960242	0.981591	0.979786	0.978161	0.009513	0.003884	0.000028	0.00388	0.010
.	.	.	.	.	.	.	.	.	.	.	.	.
.	.	.	.	.	.	.	.	.	.	.	.	.
.	.	.	.	.	.	.	.	.	.	.	.	.
65527	1.855118	1.851514	1.871255	1.817359	1.857697	1.854316	1.851210	0.017971	0.007337	0.000028	0.00734	0.019
65528	2.237246	2.232877	2.256833	2.191710	2.240453	2.236355	2.232579	0.021710	0.008863	0.000028	0.00886	0.023
65529	1.673617	1.670297	1.688168	1.639513	1.675883	1.672764	1.670040	0.016217	0.006621	0.000028	0.00662	0.017
65530	1.488124	1.485275	1.501182	1.457767	1.490262	1.487500	1.485018	0.014472	0.005908	0.000028	0.00591	0.015
65531	1.681137	1.677906	1.695874	1.646938	1.683497	1.680375	1.677621	0.016304	0.006656	0.000028	0.00666	0.017
65532	2.063357	2.059362	2.081359	2.021289	2.066161	2.062414	2.058990	0.020020	0.008173	0.000028	0.00817	0.021
65533	1.878050	1.874340	1.894466	1.839729	1.880632	1.877149	1.874061	0.018241	0.007447	0.000028	0.00745	0.019
65534	1.692556	1.689319	1.707387	1.658077	1.695011	1.691792	1.689024	0.016438	0.006711	0.000028	0.00671	0.017
65535	1.318042	1.315471	1.329608	1.291152	1.319869	1.317457	1.315266	0.012813	0.005231	0.000028	0.00523	0.013
65536	2.078676	2.074672	2.096771	2.036233	2.081482	2.077729	2.074260	0.020182	0.008239	0.000028	0.00824	0.021
Average Value	**1.68357**	**1.68030**	**1.69840**	**1.64924**	**1.68596**	**1.68285**	**[Average of the Averages = 1.680054 GPa]; [STDEV of averages, S = 0.01638 GPa]**					

A2. Polystyrene material: AFM measurement of the modulus of elasticity (GPa)

n	Replicate 1 (GPa)	Replicate 2 (GPa)	Replicate 3 (GPa)	Replicate 4 (GPa)	Replicate 5 (GPa)	Replicate 6 (GPa)	Average Value (GPa)	Standard Deviation (GPa)	u_A (GPa)	u_B (GPa)	$u_C = \sqrt{u_A^2 + u_B^2}$ (GPa)	$U = k * u_C$ (GPa)
1	3.410443	3.339803	3.482497	3.409775	3.411184	3.340857	3.399093	0.053389	0.021796	0.000028	0.021796	0.056
2	3.368394	3.298605	3.439524	3.367735	3.369126	3.299645	3.357171	0.052729	0.021527	0.000028	0.021527	0.055
3	3.346496	3.277087	3.417255	3.345841	3.347223	3.278120	3.335337	0.052447	0.021411	0.000028	0.021412	0.055
4	3.346680	3.277270	3.417347	3.346025	3.347407	3.278304	3.335506	0.052419	0.021400	0.000028	0.021400	0.055
5	3.338031	3.268902	3.408421	3.337378	3.338756	3.269933	3.326904	0.052209	0.021314	0.000028	0.021314	0.055
6	3.310152	3.241498	3.379987	3.309504	3.310871	3.242520	3.299089	0.051828	0.021159	0.000028	0.021159	0.054
7	3.310428	3.241774	3.380263	3.309780	3.311147	3.242796	3.299365	0.051828	0.021159	0.000028	0.021159	0.054
8	3.302883	3.234417	3.372625	3.302237	3.303601	3.235437	3.291867	0.051717	0.021113	0.000028	0.021113	0.054
9	3.295706	3.227428	3.365355	3.295061	3.296423	3.228446	3.284736	0.051606	0.021068	0.000028	0.021068	0.054
10	3.273808	3.205910	3.342903	3.273167	3.274519	3.206921	3.262871	0.051267	0.020930	0.000028	0.020930	0.054
.	.	.	.	.	.	.	.	.	.	.	.	.
.	.	.	.	.	.	.	.	.	.	.	.	.
.	.	.	.	.	.	.	.	.	.	.	.	.
65527	1.442717	1.412873	1.473148	1.442435	1.443030	1.413319	1.437920	0.022553	0.009207	0.000028	0.009207	0.024
65528	1.442809	1.412965	1.473240	1.442527	1.443122	1.413411	1.438012	0.022553	0.009207	0.000028	0.009207	0.024
65529	1.442717	1.412873	1.473148	1.442435	1.443030	1.413319	1.437920	0.022553	0.009207	0.000028	0.009207	0.024
65530	1.423855	1.394298	1.453916	1.423576	1.424164	1.394737	1.419091	0.022312	0.009109	0.000028	0.009109	0.023
65531	1.409869	1.380687	1.439653	1.409593	1.410176	1.381123	1.405183	0.022061	0.009006	0.000028	0.009006	0.023
65532	1.406281	1.377101	1.435880	1.406006	1.406587	1.377535	1.401565	0.022003	0.008983	0.000028	0.008983	0.023
65533	1.373433	1.345007	1.402385	1.373165	1.373732	1.345431	1.368859	0.021471	0.008765	0.000028	0.008765	0.023
65534	1.351351	1.323304	1.379840	1.351087	1.351645	1.323722	1.346825	0.021161	0.008639	0.000028	0.008639	0.022
65535	1.351351	1.323304	1.379840	1.351087	1.351645	1.323722	1.346825	0.021161	0.008639	0.000028	0.008639	0.022
65536	1.351351	1.323304	1.379840	1.351087	1.351645	1.323722	1.346825	0.021161	0.008639	0.000028	0.008639	0.022
Average Value	**2.54927**	**2.49642**	**2.60309**	**2.54878**	**2.54983**	**2.49721**	**[Average of the Averages = 2.540766 GPa]; [STDEV of averages, S = 0.039917 GPa]**					